Z. angew. Math. Phys. 51 (2000) 236–266
0044-2275/00/020236-31 $ 1.50+0.20/0

Zeitschrift für angewandte Mathematik und Physik ZAMP

Transient wave propagation in a transversely isotropic piezoelectric half space

Shaofan Li

Abstract. This work presents a systematic analysis on the transient responses of a piezoelectric half space to mixed anti-plane mechanical/in-plane electrical line sources, which is in fact the Lamb's problem for a transversely isotropic piezoelectric half space.

A key assumption of the classical piezoelectricity theory is the so-called "*quasi-static*" approximation, and it reduces the Maxwell equations to the charge equation of the electrostatics — an elliptic partial differential equation. Consequently, the dynamic piezoelectricity equations are no longer a hyperbolic system, which then poses serious difficulties in studying the transient behaviors of piezoelectric materials, a problem that has profound engineering significance. To circumvent this difficulty, a so-called "*quasi-hyperbolic*" approximation is introduced in this paper. Under this assumption, the simplified Maxwell-Christoffel equations remain as a hyperbolic system of partial differential equations.

Based on the proposed equations, two types of mixed boundary value problems have been solved: (1) anti-plane mechanical line source with boundary surface covered by a conductive film; (2) anti-plane mechanical / in-plane electric line sources with boundary surface abutted to another vacuum half space. In addition to the responses of shear-horizontal (SH) acoustic wave and transverse electric (TE) wave, the closed form solutions obtained here reveal that there exit other transient responses due to the electroacoustic surface wave—the celebrated Bleustein-Gulyaev wave, electroacoustic head wave, as well as a purely electric head wave.

Mathematics Subject Classification (1991). 35L05, 73D20, 73D25, 73R05.

Keywords. Bleustein-Gulyaev wave, Lamb's problem, Piezoelectricity, Quasi-hyperbolic approximation.

1. Introduction

The systematic study of the piezoelectricity, from theoretical and applied mechanics point of view, can be traced back at least for half a century (e.g. Cady [1946], Toupin [1956], [1963], Tiersten [1969], Auld [1973ab], Parton & Kudryatvsev [1988]), and, as a branch of physics, it has been studied for more than a century (e.g. Currie brothers [1881], Voigt [1899]) . Today, piezoelectric sensors and actuators are the most prominent transducers used in modern technologies, because they have high resolution (order of nanometer), good frequency response (order

of kHz), and generate large forces. Aerospace industrial has been implementing in large scale the integrated distributed sensor and actuator to control various flexible structures. These distributed sensors and actuators are made of predominantly piezoelectric polymer, which, as part of an adaptive control system, can sense and detect any undesirable deflections of the structures, and correct them in a "smart" fashion (Rao & Sunar [1994]).

All these applications are involved with wave propagations through the piezoelectric components, and hence, their dynamic, or transient behaviors are the primary concern in design as well as in performance. Although this is a linear problem in an established field, the surprising fact is that even today, to this author's knowledge, there are few analytical results available, if there are any correct results at all, in describing the transient behaviors of piezoelectric materials.

In this paper, an analysis is presented to study the transient behaviors of a transversely isotropic piezoelectric material – $6mm$ symmetric class – under external, anti-plane mechanical and in-plane electrical line sources, because this is a special situation that exhibits the distinct feature of piezoelectricity, which is fundamentally different from the behaviors of ordinary elasto-dielectric solids.

The main reason that transient problems for piezoelectric media are difficult to manage is because of lacking an appropriate mathematical modelling. Initially, both Maxwell equations as well as the equations of motion (elastodynamics) are hyperbolic in nature. After the quasi-static approximation—an assumption that is universally accepted, the simplified Maxwell equations, the charge equation of electrostatics, loses hyperbolicity, i.e. it becomes an elliptic type of partial differential equation. Unfortunately this simplification does not always make life easy, especially, for dynamic problems. In fact, the quasi-static approximation sacrifices the structure of the fundamental solutions of the original wave equations for mathematical simplicity. More precisely, the quasi-static approximation alters the structure of the Green's function of the coupled wave propagation problem; consequently, the solutions of the wave propagation problem based on the quasi-static approximation may not reflect the physical reality.

To remedy this deficiency caused by quasi-static approximation, in this paper, a so-called quasi-hyperbolic approximation is proposed for a class of transversely isotropic piezoelectric materials to replace the quasi-static approximation. By doing so, the newly derived governing partial differential equations of piezoelectricity recover hyperbolicity, and at the same time enjoy the simplicity that the classical piezoelectricity theory possesses.

Based on the proposed governing equations, the transient responses of a piezoelectric half space to both mechanical as well as electrical line sources are sought by integral transform method with Cagniard–de Hoop technique. Literally speaking, we are studying the Lamb's problem (Lamb [1903]) for a transversely isotropic piezoelectric medium, which is considered as one of the fundamental problems in electro-elastodynamics.

Some new and interesting results are obtained from the analysis, such as the dis-

turbances of electroacoustic surface wave, i.e. Bleustein-Gulyaev wave (Bleustein [1968], Gulyaev [1969]), the disturbances of electroacoustic head wave, and the differences as well as ramifications between mechanical surface loads and electrical surface loads. The analysis provides a sound theoretical ground for a better understanding of the transient behaviors of piezoelectric materials.

The arrangement of the paper is as follows. In section 2, the mathematical formulation of piezoelectricity theory under the quasi-hyperbolic approximation is derived in detail. Section 3 presents the solution procedures of the first type mixed boundary value problem— mechanical line source with boundary surface covered by a virtual metallic film. The second type of mixed boundary value problem, mechanical/electrical line sources with boundary surface abutted with vacuum half space, is solved in section 4.

2. Formulations of the problem

By adopting the notations in Auld [1990ab], all relevant equations of linear piezoelectricity theory are listed as follows:

(i) Maxwell's equations

$$-\nabla \times \mathbf{E} = \frac{\partial \mathbf{B}}{\partial t} \quad , \tag{2.1}$$

$$\nabla \times \mathbf{H} = \frac{\partial \mathbf{D}}{\partial t} \quad , \tag{2.2}$$

where $\mathbf{E}$, $\mathbf{B}$, and $\mathbf{H}$ are the electric field, magnetic induction, and magnetic field respectively;

(ii) Equations of motion

$$\nabla \cdot \boldsymbol{\sigma} = \rho \frac{\partial^2 \mathbf{u}}{\partial t^2} - \mathbf{F} \quad , \tag{2.3}$$

where $\boldsymbol{\sigma}$ is the Cauchy stress tensor, $\mathbf{u}$ is the displacement vector, and $\mathbf{F}$ is the body force;

(iii) Constitutive equations

$$\mathbf{B} = \mu_0 \mathbf{H} \quad , \tag{2.4}$$

$$\mathbf{D} = \boldsymbol{\epsilon}^s \cdot \mathbf{E} + \mathbf{e} : \boldsymbol{\varepsilon} \quad , \tag{2.5}$$

$$\boldsymbol{\sigma} = -\mathbf{e} \cdot \mathbf{E} + \mathbf{c}^E : \boldsymbol{\varepsilon} \quad , \tag{2.6}$$

where $\boldsymbol{\epsilon}^s$, $\mathbf{e}$, and $\mathbf{c}^E$ are the specific dielectric tensor, piezoelectric stress tensor, and elastic stiffness tensor respectively; μ_0 is the magnetic permeability constant in the vacuum.

In the constitutive equations (2.5) and (2.6), the strain tensor $\boldsymbol{\varepsilon}$ is defined as

$$\boldsymbol{\varepsilon} := \frac{1}{2}\big(\nabla\mathbf{u} + (\nabla\mathbf{u})^T\big) =: \nabla_s\mathbf{u} \tag{2.7}$$

By proper manipulation and letting the body force $\mathbf{F} = 0$, one may derive the following fully-coupled Maxwell-Christoffel equations (see Auld [1990a] page 292, Eq. (8.105) and (8.106))

$$\nabla\cdot\mathbf{c}^E \,\mathbf{:}\, \nabla_s\mathbf{u} = \rho\frac{\partial^2\mathbf{u}}{\partial t^2} + \nabla\cdot(\mathbf{e}\cdot\mathbf{E}) \quad , \tag{2.8}$$

$$-\nabla\times\nabla\times\mathbf{E} = \mu_0\boldsymbol{\epsilon}^s\cdot\frac{\partial^2\mathbf{E}}{\partial t^2} + \mu_0\mathbf{e}\,\mathbf{:}\,\nabla_s\frac{\partial^2\mathbf{u}}{\partial t^2} \quad , \tag{2.9}$$

which are a hyperbolic system.

Consider the coupling between the anti-plane acoustic mode and the in-plane electromagnetic mode, i.e. assuming,

$$\mathbf{u} = (0, 0, w(x_1, x_2, t)) \tag{2.10}$$

$$\mathbf{E} = (E_1(x_1, x_2, t), E_2(x_1, x_2, t), 0) \ . \tag{2.11}$$

The coupled wave equations (2.8) and (2.9) can be simplified drastically. For the hexagonal symmetry ($6mm$) piezoelectric material, in terms of the compressed matrix notation or Voigt notation (contrasting to the full tensor notation), Eq. (2.8) and (2.9) reduce to

$$c_{44}^E\nabla^2 w = \rho\frac{\partial^2 w}{\partial t^2} + e_{15}\nabla\cdot\mathbf{E} \quad , \tag{2.12}$$

$$-\nabla\times\nabla\times\mathbf{E} = \mu_0\epsilon_{11}^s\frac{\partial^2\mathbf{E}}{\partial t^2} + \mu_0 e_{15}\nabla\frac{\partial^2 w}{\partial t^2} \quad , \tag{2.13}$$

where the differential operator ∇ and the electric field $\mathbf{E}$ are understood as 2-D vectors, i.e.

$$\nabla := \mathbf{i}\frac{\partial}{\partial x_1} + \mathbf{j}\frac{\partial}{\partial x_2} \tag{2.14}$$

$$\mathbf{E} := E_1\mathbf{i} + E_2\mathbf{j} \ . \tag{2.15}$$

Let

$$\mathbf{E} = -\nabla\phi - \frac{1}{c_\ell}\frac{\partial\mathbf{A}}{\partial t} \ , \tag{2.16}$$

where ϕ and $\mathbf{A}$ are a scalar potential and a vector potential respectively, and the constant, $c_\ell := (\mu_0\epsilon_{11}^s)^{-1/2}$, is the speed of light in the piezoelectric medium.

The decomposition (2.16) can be uniquely determined by imposing the following Lorentz gauge within the transversely isotropic plane,

$$\nabla \cdot \mathbf{A} + \frac{1}{c_\ell}\frac{\partial \phi}{\partial t} = 0 \ . \tag{2.17}$$

Subsequently, the coupled wave equations (2.12), (2.13) can be further split into two groups, namely,

(a) The purely electro-acoustic wave equations,

$$\begin{cases} c_{44}^E \nabla^2 w - \rho \dfrac{\partial^2 w}{\partial t^2} = -e_{15}\left(\nabla^2 \phi - \dfrac{1}{{c_\ell}^2}\dfrac{\partial^2 \phi}{\partial t^2}\right) \ , \\ \dfrac{e_{15}}{\epsilon_{11}^s}\nabla^2 w = \left(\nabla^2 \phi - \dfrac{1}{{c_\ell}^2}\dfrac{\partial^2 \phi}{\partial t^2}\right) \ ; \end{cases} \tag{2.18}$$

(b) The rotational part of electromagneto-acoustic wave equations,

$$\begin{cases} \nabla^2 A_1 - \dfrac{1}{{c_\ell}^2}\dfrac{\partial^2 A_1}{\partial t^2} = -\mu_0 e_{15} c_\ell \dfrac{\partial^2 w}{\partial t \partial x_1} \ , \\ \nabla^2 A_2 - \dfrac{1}{{c_\ell}^2}\dfrac{\partial^2 A_2}{\partial t^2} = -\mu_0 e_{15} c_\ell \dfrac{\partial^2 w}{\partial t \partial x_2} \ . \end{cases} \tag{2.19}$$

Define

$$\bar{c}_{44} := c_{44}^E + \frac{{e_{15}}^2}{\epsilon_{11}^s} \ , \tag{2.20}$$

$$c_s := \left(\frac{\bar{c}_{44}}{\rho}\right)^{1/2} \ , \tag{2.21}$$

$$C_f := \frac{{c_\ell}^2}{{c_\ell}^2 - c_s^2} \ ; \tag{2.22}$$

and introduce a new scalar potential function ψ,

$$\boxed{\psi := \phi - \frac{e_{15}}{\epsilon_{11}^s} C_f w} \ . \tag{2.23}$$

Accordingly, the relevant constitutive equations can be expressed in terms of w, ψ, and A_i,

$$\sigma_{13} = \tilde{c}_{44}\frac{\partial w}{\partial x_1} + e_{15}\frac{\partial \psi}{\partial x_1} + \frac{e_{15}}{c_\ell}\frac{\partial A_1}{\partial t} \tag{2.24}$$

$$\sigma_{23} = \tilde{c}_{44}\frac{\partial w}{\partial x_2} + e_{15}\frac{\partial \psi}{\partial x_2} + \frac{e_{15}}{c_\ell}\frac{\partial A_2}{\partial t} \tag{2.25}$$

$$D_1 = e_{15}(1 - C_f)\frac{\partial w}{\partial x_1} - \epsilon_{11}^s \frac{\partial \psi}{\partial x_1} - \frac{\epsilon_{11}^s}{c_\ell}\frac{\partial A_1}{\partial t} \tag{2.26}$$

$$D_2 = e_{15}(1 - C_f)\frac{\partial w}{\partial x_2} - \epsilon_{11}^s \frac{\partial \psi}{\partial x_2} - \frac{\epsilon_{11}^s}{c_\ell}\frac{\partial A_2}{\partial t} \tag{2.27}$$

where $\tilde{c}_{44} := \bar{c}_{44} - (1 - C_f){e_{15}}^2/\epsilon_{11}^s$.

Furthermore, the purely electro-acoustic wave equations (2.18) can be completely decoupled as follows,

$$\boxed{\begin{cases} \nabla^2 w - \dfrac{1}{c_s^2}\dfrac{\partial^2 w}{\partial t^2} = 0 \ , & (a) \\ \nabla^2 \psi - \dfrac{1}{{c_\ell}^2}\dfrac{\partial^2 \psi}{\partial t^2} = 0 \ . & (b) \end{cases}} \tag{2.28}$$

In most piezoelectric materials, the induced magnetic field is negligible. From this standpoint, the quasi-static approximation (See: Tiersten [1969] page 30) assumes that the rotational part of the electric field satisfies the condition

$$\left| \ \dot{A}_i/c_\ell \ \right| << \left| \ \phi_{,i} \ \right| \tag{2.29}$$

Since each time derivative of A_i is supposedly bringing down a factor of c_ℓ, condition (2.29) suggests the following asymptotic estimate

$$|A_i| \sim \mathcal{O}\Big(\frac{\phi}{c_\ell}\Big), \text{ or } \mathcal{O}\Big(\frac{w}{c_\ell}\Big) \tag{2.30}$$

where $c_\ell^{-1} << 1$ is chosen as the perturbation parameter.

Since the vector potential $\mathbf{A}$ is a higher order term, in the zero-th order approximation, the rotational part of the governing equations (2.19) can be neglected. Note that $\mu_0 e_{15} c_\ell \sim 1/c_\ell$ in (2.19) .

In addition, the quasi-static approximation further assumes that

$$c_\ell \to \infty, \ C_f \to 1 \tag{2.31}$$

It then recovers the classical equations for linear piezoelectric materials of $6mm$ symmetry class in transverse space, i.e.

$$\nabla^2 w - \frac{1}{c_s^2}\frac{\partial^2 w}{\partial t^2} = 0 \ , \tag{2.32}$$

$$\nabla^2 \psi = 0 \ . \tag{2.33}$$

and

$$\sigma_{13} = \bar{c}_{44}\frac{\partial w}{\partial x_1} + e_{15}\frac{\partial \psi}{\partial x_1} \tag{2.34}$$

$$\sigma_{23} = \bar{c}_{44}\frac{\partial w}{\partial x_2} + e_{15}\frac{\partial \psi}{\partial x_2} \tag{2.35}$$

$$D_1 = -\epsilon_{11}^s\frac{\partial \psi}{\partial x_1} \tag{2.36}$$

$$D_2 = -\epsilon_{11}^s\frac{\partial \psi}{\partial x_2} \tag{2.37}$$

One may notice that Eq. (2.33) has lost hyperbolicity. To remedy this deficiency, we discard the conventional "quasi-static" approximation, and adopt the following "quasi-hyperbolic" approximation:

Assumption 2.1. (Quasi-hyperbolic approximation). *The so-called "quasi-hyperbolic" approximation assumes:*

(i) The rotational electric field is neglected;

(ii) The light speed is finite; □

Technically speaking, after asymptotic analysis, the quasi-hyperbolic assumption only discards Eq. (2.19) and the terms involved with A_i in (2.24)–(2.27), but keeps Eq.(2.18), or Eq.(2.28(a),(b)) intact. The governing equations of piezoelectricity in the transversely isotropic space, formulated under quasi-hyperbolic approximation, are Eqs. (2.23), (2.28), and

$$\boxed{\begin{aligned} \sigma_{13} &= \tilde{c}_{44}\frac{\partial w}{\partial x_1} + e_{15}\frac{\partial \psi}{\partial x_1} && (a)\\ \sigma_{23} &= \tilde{c}_{44}\frac{\partial w}{\partial x_2} + e_{15}\frac{\partial \psi}{\partial x_2} && (b)\\ D_1 &= e_{15}(1-C_f)\frac{\partial w}{\partial x_1} - \epsilon_{11}^s\frac{\partial \psi}{\partial x_1} && (c)\\ D_2 &= e_{15}(1-C_f)\frac{\partial w}{\partial x_2} - \epsilon_{11}^s\frac{\partial \psi}{\partial x_2} && (d) \end{aligned}} \tag{2.38}$$

which are highlighted by fitting them into a box.

Remark 2.1. (**1.**) Both quasi-static approximation and quasi-hyperbolic approximation are zero-th order approximation, but by including some higher order terms in Eq.(2.28(a),(b)) we restore the hyperbolicity into the simplified system.

(**2.**) Without adopting any approximation, some exact solutions of surface waves on piezoelectric half space are given in Li [1996], which, on the other hand, has shown how involved it could be by taking into the full account of electromagnetic effect.

(**3.**) Under quasi-hyperbolic approximation, the electromagneto-acoustic wave problem in the transversely isotropic piezoelectric space degenerates to the coupling problem between the shear-horizontal (SH) acoustic wave and the transverse electric (TE) wave, or simply *electric wave* (Jackson [1974] page 342). □

For the sake of consistency, the above assumption is also applied to the other dielectric media that are within the same environment as the piezoelectric medium under the consideration. For instance, if the piezoelectric medium is in contact with a free space, the rotational part of electromagnetic field in the vacuum space is also neglected, and the simplified Maxwell equations in the free space are then

reduced to a single wave equation instead of Laplace equation under the quasi-static approximation, namely

$$\boxed{\nabla^2\tilde{\phi} - \frac{1}{c_0^2}\frac{\partial^2\tilde{\phi}}{\partial t^2} = 0} \tag{2.39}$$

where $c_0 = (\mu_0\epsilon_0)^{-1/2}$ is the light speed in the vacuum.

Since electromagnetic field is ubiquitous, all the boundaries are in fact interfaces. The corresponding prescribed boundary conditions are then imposed as the standard form in continuum mechanics (e.g. Achenbach [1973]) and electrodynamics (e.g. Jackson [1974], Felsen & Marcuvitz [1994]),

$$\mathbf{n}\cdot[|\boldsymbol{\sigma}|] = \mathbf{T}_0\ ,\ \mathbf{x}\in\partial\Omega_\sigma \tag{2.40}$$

$$\mathbf{u} = \bar{\mathbf{u}}\ ,\ \mathbf{x}\in\partial\Omega_u \tag{2.41}$$

$$\mathbf{n}\cdot[|\mathbf{D}|] = q_0\ ,\ \mathbf{x}\in\partial\Omega_D \tag{2.42}$$

$$\mathbf{n}\times[|\mathbf{E}|] = 0\ ,\ \mathbf{x}\in\partial\Omega_E \tag{2.43}$$

Note that $\partial\Omega_\sigma\cap\partial\Omega_u = \emptyset$, but $\partial\Omega_D\cap\partial\Omega_E \neq \emptyset$.

In addition, it is assumed that the displacement field w as well as the electrical scalar potential ϕ have the quiescent history before the line sources are applied, i.e., $\forall t < 0$

$$w(x_1,x_2,t) = \dot{w}(x_1,x_2,t) = 0 \tag{2.44}$$

$$\phi(x_1,x_2,t) = \dot{\phi}(x_1,x_2,t) = 0 \tag{2.45}$$

$$\tilde{\phi}(x_1,x_2,t) = \dot{\tilde{\phi}}(x_1,x_2,t) = 0 \tag{2.46}$$

3. Lamb's problem with shielded surface

(a) Transform solutions

In piezoelectric media, field variables consist of both mechanical variables as well as electric variables. Hence, the term "*Lamb's problem* used here is in a generalized sense, namely, a half space problem with line sources. In particular, the Lamb's problem with shielded surface is referred to as a half space problem in which the surface of the piezoelectric half space is covered with a virtual, conductive thin sheet, i.e. having a short-circuit boundary as shown in Figure (1). Mathematically it reads as

$$\begin{cases} \sigma_{23}(x_1,0,t) = -\sigma_0\delta(x_1)F(t)\ ;\ t>0 \\ \phi(x_1,0,t) = 0\ ;\ t>0 \end{cases} \tag{3.1}$$

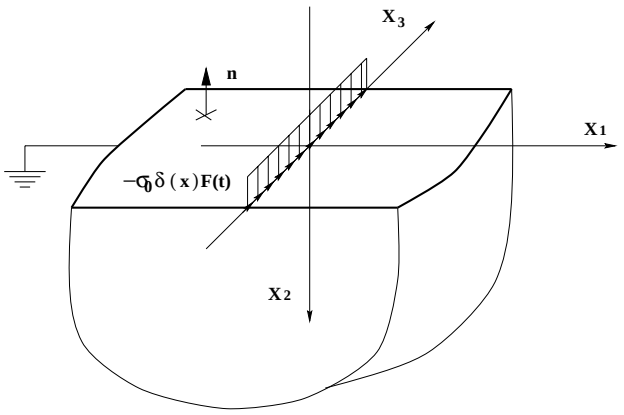

Figure 1.
Mechanical line source applying to a piezoelectric half space with short-circuit surface

Applying the following unilateral and bilateral Laplace transforms to a function, $f(x,t)$,

$$\begin{cases} f^*(x,p) = \displaystyle\int_0^\infty f(x,t)\exp(-pt)dt \\ f(x,t) = \dfrac{1}{2\pi i}\displaystyle\int_{p_0-i\infty}^{p_0+i\infty} f^*(x,p)\exp(pt)dp \end{cases} \tag{3.2}$$

$$\begin{cases} \hat{f}^*(\zeta,p) = \displaystyle\int_{-\infty}^\infty f^*(x,p)\exp(-p\zeta x)dx \\ f^*(x,p) = \dfrac{p}{2\pi i}\displaystyle\int_{\zeta_0-i\infty}^{\zeta_0+i\infty} \hat{f}^*(\zeta,p)\exp(p\zeta x)d\zeta \end{cases} \tag{3.3}$$

The wave equations (2.28(a)), (2.28(b)) become

$$\Big(\frac{d^2}{dx_2^2} - p^2a^2(\zeta)\Big)\hat{w}^*(\zeta,x_2,p) = 0 \tag{3.4}$$

$$\Big(\frac{d^2}{dx_2^2} - p^2e^2(\zeta)\Big)\hat{\psi}^*(\zeta,x_2,p) = 0 \tag{3.5}$$

where $a(\zeta) = \sqrt{s_s^2-\zeta^2}$, $e(\zeta) = \sqrt{s_\ell^2-\zeta^2}$ and the slownesses $s_s := 1/c_s$, $s_\ell := 1/c_\ell$.

The relevant solutions are

$$\hat{w}^*(\zeta,x_2,p) = A(\zeta,p)\exp(-pa(\zeta)x_2)\ ,\ a(\zeta) := \sqrt{s_s^2-\zeta^2}\ ; \tag{3.6}$$

$$\hat{\psi}^*(\zeta,x_2,p) = B(\zeta,p)\exp(-pe(\zeta)x_2)\ ,\ e(\zeta) := \sqrt{s_\ell^2-\zeta^2}\ ; \tag{3.7}$$

From the transformed boundary conditions,

$$\hat{\sigma}^*_{32}(\zeta,0,p) = -p\Big[\tilde{c}_{44}a(\zeta)A(\zeta,p) + e_{15}e(\zeta)B(\zeta,p)\Big] = -\sigma_0 F^*(p) \tag{3.8}$$

$$\hat{\psi}^*(\zeta,0,p) = \frac{e_{15}}{\epsilon^s_{11}}C_f A(\zeta,p) + B(\zeta,p) = 0\ , \tag{3.9}$$

one can derive that

$$A(\zeta,p) = \Big(\frac{\sigma_0}{\tilde{c}_{44}}\Big)\Big(\frac{F^*(p)/p}{(1-k_e^4)}\Big)\frac{[a(\zeta)+k_e^2 e(\zeta)]}{(s_{bge}+\zeta)(s_{bge}-\zeta)} \tag{3.10}$$

$$B(\zeta,p) = -\frac{e_{15}}{\epsilon^s_{11}}C_f A(\zeta,p) \tag{3.11}$$

where $s_{bge} := \sqrt{\dfrac{s_s^2 - k_e^4 s_\ell^2}{1-k_e^4}}$, $k_e^2 := \dfrac{{e_{15}}^2}{\epsilon^s_{11}\tilde{c}_{44}}C_f$, and $c_{bge} = 1/s_{bge}$.

Remark 3.1.

(**1**) Take $c_\ell \to \infty$ ($s_\ell \to 0$). Then $C_f \to 1$, $k_e^2 \to {e_{15}}^2/(\epsilon^s_{11}\tilde{c}_{44})$, and

$$c_{bge} \to c_s\sqrt{1-k_e^4} \tag{3.12}$$

which is the expression of the Bleustein-Gulyaev wave speed in classical piezoelectric theory with short-circuit electric boundary condition.

(**2**) Define Bleustein-Gulyaev function

$$BG(\zeta) := a(\zeta) - k_e^2 e(\zeta)\ . \tag{3.13}$$

The Bleustein-Gulyaev function was first introduced by Li & Mataga (Li & Mataga [1996]). As shown in Appendix A,[†] the Bleustein-Gulyaev function can be further decomposed as

$$BG(\zeta) = (1-k_e^2)\frac{(s_{bge}+\zeta)(s_{bge}-\zeta)}{\sqrt{(s_s+\zeta)(s_s-\zeta)}}\mathcal{S}_+(\zeta)\mathcal{S}_-(\zeta) \tag{3.14}$$

where

$$\mathcal{S}_\pm(\zeta) = \exp\left\{\frac{1}{\pi}\int_{s_\ell}^{s_s}\arctan\left[\frac{k_e^2\sqrt{(\eta-s_\ell)(\eta+s_\ell)}}{\sqrt{(s_s-\eta)(s_s+\eta)}}\right]\frac{d\eta}{\eta\pm\zeta}\right\}\ . \tag{3.15}$$

□

[†] There is sign error in Li & Mataga [1996ab]

The full set of integral representations of the field variables are as follows

$$w^*(x_1,x_2,p)=\frac{p}{2\pi i}\int_{\zeta_a-i\infty}^{\zeta_a+i\infty}A(\zeta,p)\exp[-p(a(\zeta)x_2-\zeta x_1)]d\zeta \tag{3.16}$$

$$\begin{aligned}\phi^*(x_1,x_2,p)=\frac{p}{2\pi i}\frac{e_{15}}{\epsilon_{11}^s}C_f\Bigg\{&\int_{\zeta_a-i\infty}^{\zeta_a+i\infty}A(\zeta,p)\exp[-p(a(\zeta)x_2-\zeta x_1)]d\zeta\\&-\int_{\zeta_e-i\infty}^{\zeta_e+i\infty}A(\zeta,p)\exp[-p(e(\zeta)x_2-\zeta x_1)]d\zeta\Bigg\}\end{aligned} \tag{3.17}$$

and

$$\begin{aligned}\sigma_{31}^*(x_1,x_2,p)=\frac{\tilde{c}_{44}p^2}{2\pi i}\Bigg\{&\int_{\zeta_a-i\infty}^{\zeta_a+i\infty}\zeta A(\zeta,p)\exp[-p(a(\zeta)x_2-\zeta x_1)]d\zeta\\&-k_e^2\int_{\zeta_e-i\infty}^{\zeta_e+i\infty}\zeta A(\zeta,p)\exp[-p(e(\zeta)x_2-\zeta x_1)]d\zeta\Bigg\}\end{aligned} \tag{3.18}$$

$$\begin{aligned}\sigma_{32}^*(x_1,x_2,p)=-\frac{\tilde{c}_{44}p^2}{2\pi i}\Bigg\{&\int_{\zeta_a-i\infty}^{\zeta_a+i\infty}a(\zeta)A(\zeta,p)\exp[-p(a(\zeta)x_2-\zeta x_1)]d\zeta\\&-k_e^2\int_{\zeta_e-i\infty}^{\zeta_e+i\infty}e(\zeta)A(\zeta,p)\exp[-p(e(\zeta)x_2-\zeta x_1)]d\zeta\Bigg\}\end{aligned} \tag{3.19}$$

$$\begin{aligned}D_1^*(x_1,x_2,p)=\frac{e_{15}fp^2}{2\pi i}\Bigg\{&(1-C_f)\int_{\zeta_a-i\infty}^{\zeta_a+i\infty}\zeta A(\zeta,p)\exp[-p(a(\zeta)x_2-\zeta x_1)]d\zeta\\&+C_f\int_{\zeta_e-i\infty}^{\zeta_e+i\infty}\zeta A(\zeta,p)\exp[-p(e(\zeta)x_2-\zeta x_1)]d\zeta\Bigg\}\end{aligned} \tag{3.20}$$

$$\begin{aligned}D_2^*(x_1,x_2,p)=-\frac{e_{15}fp^2}{2\pi i}\Bigg\{&(1-C_f)\int_{\zeta_a-i\infty}^{\zeta_a+i\infty}a(\zeta)A(\zeta,p)\exp[-p(a(\zeta)x_2-\zeta x_1)]d\zeta\\&+C_f\int_{\zeta_e-i\infty}^{\zeta_e+i\infty}e(\zeta)A(\zeta,p)\exp[-p(e(\zeta)x_2-\zeta x_1)]d\zeta\Bigg\}\end{aligned} \tag{3.21}$$

where $-s_\ell<\zeta_a,\zeta_e<s_\ell$.

(b) Cagniard-de Hoop inversion

The conventional Cagniard-de Hoop technique (Cagniard [1939], de Hoop [1960]) is adopted in inversion.

Three different inversion paths are shown in Figure (2): $\Gamma_a,\Gamma_{ae},\Gamma_e$, in which

$$\begin{aligned}&a(\zeta)x_2-\zeta x_1=t\ ,\ \zeta\in\Gamma_a,\Gamma_{ae}\\&e(\zeta)x_2-\zeta x_1=t\ ,\ \zeta\in\Gamma_e\end{aligned} \tag{3.22}$$

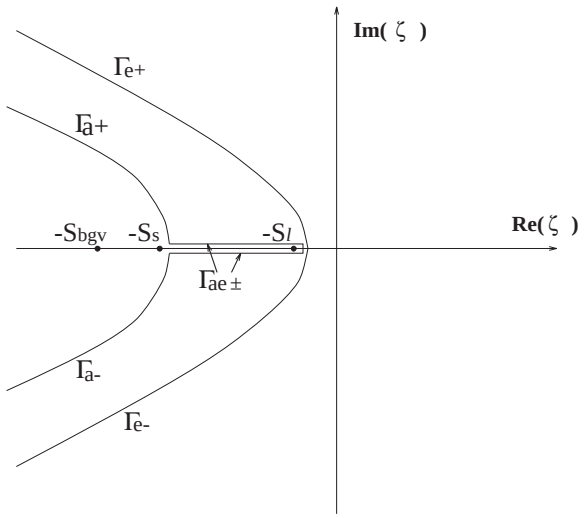

Figure 2.
Cagniard-de Hoop inversion paths for the Lamb's problem with shielded surface

Remark 3.2. It should be noted that at $\zeta = -s_s \cos\theta$, path Γ_a intercepts the real axis $Re(\zeta)$. Thus, a supplement path Γ_{ae} is needed to circumvent the branch cut of multivalued function $e(\zeta) = \sqrt{s_\ell^2 - \zeta^2}$. This, in turn, represents an electroacoustic head wave, which has no counterpart in purely elastic media. Indeed, the physical presence of such type electroacoustic head waves has been experimentally confirmed by Lin et al. (1989).

Along path Γ_{ae}, $-s_s \cos\theta \le \zeta \le -s_\ell$, there is a restraint on θ,

$$0 \le \theta \le \theta_{cr}^{ae} \ , \ \text{or } \pi \le \theta \le \pi - \theta_{cr}^{ae} \tag{3.23}$$

where $\theta_{cr}^{ae} := \cos^{-1}\Big(s_\ell / s_s\Big)$. Since $s_\ell / s_s \sim 10^{-5}$, $\theta \to \pi/2$, which suggests that the electroacoustic head wave almost propagates in parallel with the boundary surface as shown in Figure (3). In Figure (3), the region, H_{ea} is where the electroacoustic head wave sweeps through. □

Let $x_1 = r\cos\theta$, $x_2 = r\sin\theta$. One then has

$$\zeta_{a\pm} = \frac{1}{r}[-t\cos\theta \pm i\sin\theta\sqrt{t^2 - s_s^2 r^2}] \ , \ s_s r \le t < \infty \tag{3.24}$$

$$\zeta_{ae\pm} = \frac{1}{r}[-t\cos\theta \pm i\sin\theta\sqrt{s_s^2 r^2 - t^2}] \pm i\epsilon \ , \ t_{ab} \le t < s_s r \tag{3.25}$$

$$\zeta_{e\pm} = \frac{1}{r}[-t\cos\theta \pm i\sin\theta\sqrt{t^2 - s_\ell^2 r^2}] \ , \ s_\ell r \le t < \infty \tag{3.26}$$

where $t_{ae} = \sqrt{s_s^2 - s_\ell^2}\, x_2 + s_\ell x_1$.

Following de Hoop (1960), one may show that

$$\frac{\partial \zeta_{a\pm}}{\partial t} = \frac{\pm i a(\zeta_{a\pm})}{\sqrt{t^2 - s_s^2 r^2}} \; ; \; a(\zeta_{a\pm}) = \frac{\sin\theta}{r} t \pm i \frac{\cos\theta}{r} \sqrt{t^2 - s_s^2 r^2} \; ; \tag{3.27}$$

$$\frac{\partial \zeta_{ae\pm}}{\partial t} = \frac{\mp a(\zeta_{ae\pm})}{\sqrt{s_s^2 r^2 - t^2}} \; ; \; a(\zeta_{ae\pm}) = \frac{\sin\theta}{r} t \pm \frac{\cos\theta}{r} \sqrt{s_s^2 r^2 - t^2} \; ; \tag{3.28}$$

$$\frac{\partial \zeta_{e\pm}}{\partial t} = \frac{\pm i e(\zeta_{e\pm})}{\sqrt{t^2 - s_\ell^2 r^2}} \; ; \; e(\zeta_{e\pm}) = \frac{\sin\theta}{r} t \pm i \frac{\cos\theta}{r} \sqrt{t^2 - s_\ell^2 r^2} \; ; \tag{3.29}$$

and subsequently,

$$\begin{aligned} w^*(x_1, x_2, p) = & \Big(\frac{\sigma_0}{\tilde{c}_{44}}\Big)\Big(\frac{F^*(p)}{1 - k_e^4}\Big)\frac{1}{\pi} \cdot \\ & \Big\{ \int_{s_s r}^{\infty} Re\Big(\frac{a(\zeta) + k_e^2 e(\zeta)}{(s_{bge} + \zeta)(s_{bge} - \zeta)} \frac{a(\zeta)}{\sqrt{t^2 - s_s^2 r^2}} \Big) \Big|_{\zeta \in \Gamma_{a+}} \exp(-pt) dt \\ & - \int_{t_{ae}}^{s_s r} Im\Big(\frac{a(\zeta) + k_e^2 e(\zeta)}{(s_{bge} + \zeta)(s_{bge} - \zeta)} \frac{a(\zeta)}{\sqrt{s_s^2 r^2 - t^2}} \Big) \Big|_{\zeta \in \Gamma_{ae+}} \exp(-pt) dt \Big\} \end{aligned} \tag{3.30}$$

and

$$\begin{aligned} \phi^*(x_1, x_2, p) = & \Big(\frac{e_{15}}{\epsilon_{11}^s} f\Big)\Big(\frac{\sigma_0}{\tilde{c}_{44}}\Big)\Big(\frac{F^*(p)}{1 - k_e^4}\Big)\frac{1}{\pi} \cdot \\ & \Big\{ \int_{s_s r}^{\infty} Re\Big(\frac{a(\zeta) + k_e^2 e(\zeta)}{(s_{bge} + \zeta)(s_{bge} - \zeta)} \frac{a(\zeta)}{\sqrt{t^2 - s_s^2 r^2}} \Big) \Big|_{\zeta \in \Gamma_{a+}} \exp(-pt) dt \\ & - \int_{t_{ae}}^{s_s r} Im\Big(\frac{a(\zeta) + k_e^2 e(\zeta)}{(s_{bge} + \zeta)(s_{bge} - \zeta)} \frac{a(\zeta)}{\sqrt{s_s^2 r^2 - t^2}} \Big) \Big|_{\zeta \in \Gamma_{ae+}} \exp(-pt) dt \\ & - \int_{s_\ell r}^{\infty} Re\Big(\frac{a(\zeta) + k_e^2 e(\zeta)}{(s_{bge} + \zeta)(s_{bge} - \zeta)} \frac{e(\zeta)}{\sqrt{t^2 - s_\ell^2 r^2}} \Big) \Big|_{\zeta \in \Gamma_{e+}} \exp(-pt) dt \Big\} \end{aligned} \tag{3.31}$$

In this study, we are mainly interested in impulsive loading, namely, $F(t) = \delta(t)$, because the responses of arbitrarily time dependent line sources can be always represented by the following superpositions:

$$w(x_1, x_2, t) = \int_0^t w^\delta(x_1, x_2, \tau) F(t - \tau) d\tau \tag{3.32}$$

$$\phi(x_1, x_2, t) = \int_0^t \phi^\delta(x_1, x_2, \tau) F(t - \tau) d\tau \tag{3.33}$$

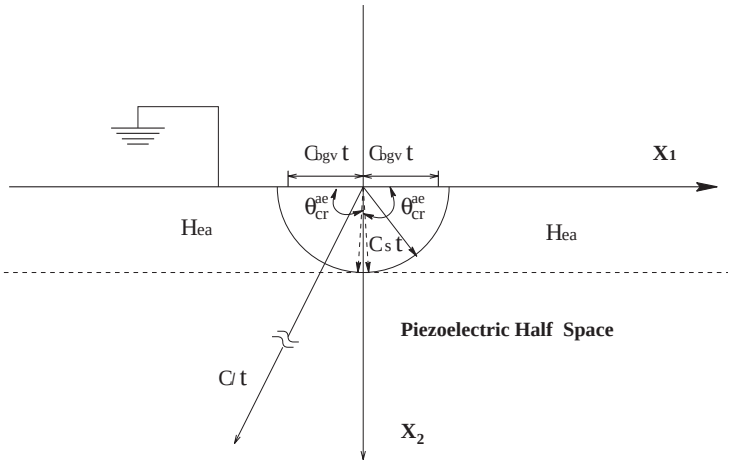

Figure 3.
The transient wave patterns in the shielded half space

where the superscript "δ" represents the transient response due to impulsive line loads.

As shown in (3.30) and (3.31), in this case, the transient waves of displacement and electrical potential can be distinguished from three different sources,

$$w^{\delta}(x_1, x_2, t) = w_a^{\delta}(x_1, x_2, t) + w_{eah}^{\delta}(x_1, x_2, t) \tag{3.34}$$

$$\phi^{\delta}(x_1, x_2, t) = \phi_a^{\delta}(x_1, x_2, t) + \phi_{eah}^{\delta}(x_1, x_2, t) + \phi_e^{\delta}(x_1, x_2, t) \tag{3.35}$$

in which, subscript "a" stands for acoustic contribution, "eah" stands for the contribution from the electroacoustic head wave, and subscript "e" stands for the contribution from the electric wave.

Specifically, in this example,

$$w_a^{\delta}(x_1, x_2, t) = \Big(\frac{\sigma_0}{\tilde{c}_{44}}\Big)\Big[\frac{H(t - s_s r)}{\pi(1 - k_e^4)}\Big] \cdot Re\Big(\frac{a(\zeta) + k_e^2 e(\zeta)}{(s_{bge} + \zeta)(s_{bge} - \zeta)} \frac{a(\zeta)}{\sqrt{t^2 - s_s r^2}}\Big)\Big|_{\zeta \in \Gamma_{a+}} \tag{3.36}$$

$$w_{eah}^{\delta}(x_1, x_2, t) = -\Big(\frac{\sigma_0}{\tilde{c}_{44}}\Big)\Big[\frac{H(t - t_{ae}) - H(t - s_s r)}{\pi(1 - k_e^4)}\Big] \cdot Im\Big(\frac{a(\zeta) + k_e^2 e(\zeta)}{(s_{bge} + \zeta)(s_{bge} - \zeta)} \frac{a(\zeta)}{\sqrt{s_s r^2 - t^2}}\Big)\Big|_{\zeta \in \Gamma_{ae+}} \tag{3.37}$$

and

$$\phi_a^\delta(x_1,x_2,t)=\Big(\frac{e_{15}}{\epsilon_{11}^s}C_f\Big)\Big(\frac{\sigma_0}{\tilde{c}_{44}}\Big)\Big[\frac{H(t-s_sr)}{\pi(1-k_e^4)}\Big]$$
$$\cdot\, Re\Big(\frac{a(\zeta)+k_e^2e(\zeta)}{(s_{bge}+\zeta)(s_{bge}-\zeta)}\frac{a(\zeta)}{\sqrt{t^2-s_sr^2}}\Big)\Big|_{\zeta\in\Gamma_{a+}} \tag{3.38}$$

$$\phi_{eah}^\delta(x_1,x_2,t)=-\Big(\frac{e_{15}}{\epsilon_{11}^s}C_f\Big)\Big(\frac{\sigma_0}{\tilde{c}_{44}}\Big)\Big[\frac{H(t-t_{ae})-H(t-s_sr)}{\pi(1-k_e^4)}\Big]$$
$$\cdot\, Im\Big(\frac{a(\zeta)+k_e^2e(\zeta)}{(s_{bge}+\zeta)(s_{bge}-\zeta)}\frac{a(\zeta)}{\sqrt{s_sr^2-t^2}}\Big)\Big|_{\zeta\in\Gamma_{ae+}} \tag{3.39}$$

$$\phi_e^\delta(x_1,x_2,t)=-\Big(\frac{e_{15}}{\epsilon_{11}^s}C_f\Big)\Big(\frac{\sigma_0}{\tilde{c}_{44}}\Big)\Big[\frac{H(t-s_\ell r)}{\pi(1-k_e^4)}\Big]$$
$$\cdot\, Re\Big(\frac{a(\zeta)+k_e^2e(\zeta)}{(s_{bge}+\zeta)(s_{bge}-\zeta)}\frac{e(\zeta)}{\sqrt{t^2-s_\ell^2r^2}}\Big)\Big|_{\zeta\in\Gamma_{e+}} \tag{3.40}$$

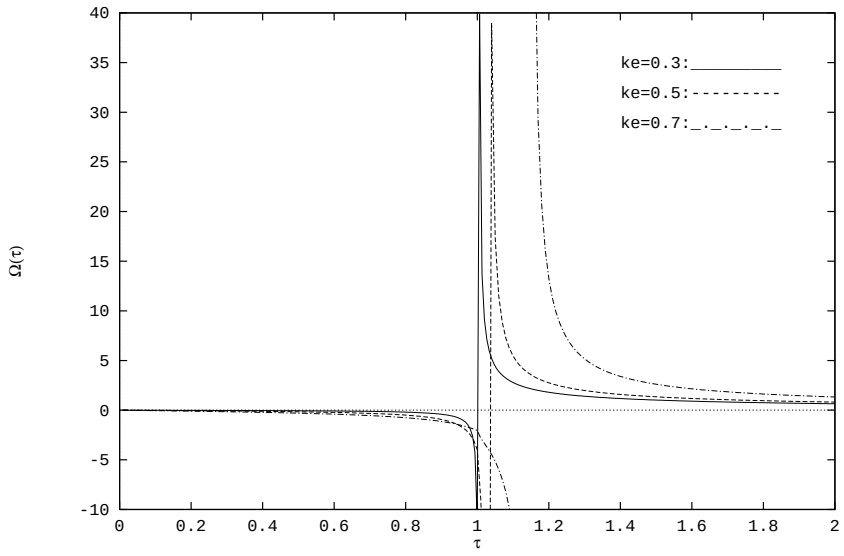

Figure 4.
The disturbance of surface displacement. $\Big(\Omega(\tau):=\frac{\tilde{c}_{44}\pi x_1}{\sigma_0 c_s}w^\delta(x_1,0,t)\Big)$

Let

$$\tau:=\frac{c_st}{x_1}\ ,\ \tau_{bge}:=\frac{s_{bge}}{s_s}=\frac{1}{\sqrt{1-k_e^4}}\ ,\ \tau_\ell:=\frac{s_\ell}{s_s}=\frac{c_s}{c_\ell}\ . \tag{3.41}$$

The transient response of displacement field on the surface $x_2 = 0$ can be expressed as

$$\frac{\tilde{c}_{44}\pi x_1}{\sigma_0 c_s} w^{\delta}(x_1, 0, t) = -\frac{1}{1-k_e^4}\left\{ \frac{\sqrt{\tau^2-1}}{(\tau_{bge}+\tau)(\tau_{bge}-\tau)} H(\tau-1) + \frac{k_e^2\sqrt{\tau^2-\tau_\ell^2}}{(\tau_{bge}+\tau)(\tau_{bge}-\tau)} H(\tau-\tau_\ell) \right\} \tag{3.42}$$

which is plotted in Figure (4) with different electro-mechanical coupling coefficient k_e. One may also verify that at $x_2 = 0$, $\phi^{\delta}(x_1, 0, t) \equiv 0$.

It should be noted that when $x_2 = 0$ there is a simple pole $\zeta = -s_{bge}$ along the integration paths $\Gamma_{a\pm}$ and $\Gamma_{e\pm}$, the integrations (3.30) and (3.31) should be understood as the Cauchy principle value, and the simple pole contribution is due to the effect of the electroacoustic surface wave—Bleustein-Gulyaev wave, which can be calculated by residual theorem. In an analogy to the Rayleigh wave, this simple pole contribution represents an impulsive surface disturbance that is nondecaying and does not change shape. In this particular case, however, the simple pole lies on an unphysical Riemann sheet, and its contribution to the displacement field is zero, because

$$\lim_{\zeta\to -s_{bge}} Re\left\{ 2\pi i(\zeta + s_{bge}) \Big[\frac{a(\zeta) + k_e^2 e(\zeta)}{(s_{bge}+\zeta)(s_{bge}-\zeta)} \begin{Bmatrix} a(\zeta) \\ e(\zeta) \end{Bmatrix} \Big] \Big|_{\zeta=-s_{bge}} \right\} = 0 \ , \tag{3.43}$$

which means that there is no impulsive singular surface disturbances for both displacement and electrical potential. On the other hand, the BG surface wave has the potential to create the leaky mode, if the boundary conditions across the interface are slightly altered.

As shown in Eq.(3.42), the singularity of the surface displacement disturbance due to Bleustein-Gulyaev wave is at order $O((\tau - \tau_{bge})^{-1})$, which is the reminiscence of Rayleigh disturbance in vertical surface displacement mode in purely elastic half space (Miklowitz [1978]).

Nevertheless, the impulsive Bleustein-Gulyaev disturbance can still be felt in other situations. Consider the step loading $F(t) = H(t)$. From Eq.(3.21), one may find that the transient response of electric displacement component D_2 on

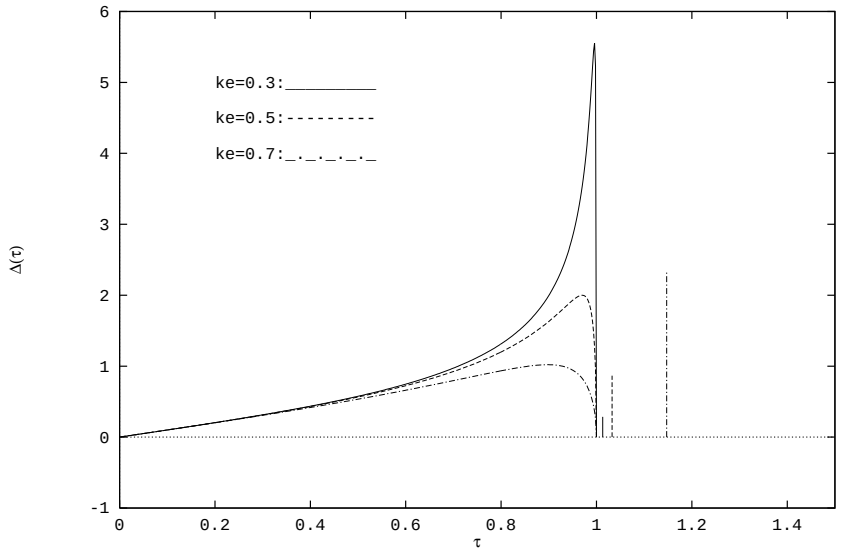

Figure 5.
The disturbance of the electric displacement on the surface. ($\Delta(\tau) := \frac{\tilde{c}_{44}\pi x_1}{\sigma_0 e_{15}} D_2(x_1, 0, t)$)

the surface is as follows

$$\frac{\tilde{c}_{44}\pi x_1}{\sigma_0 e_{15}} D_2(x_1,0,t) = \frac{1}{1-k_e^4}\left\{(1-C_f)\frac{k_e^2\sqrt{\tau^2-\tau_\ell^2}\sqrt{1-\tau^2}}{(\tau_{bge}+\tau)(\tau_{bge}-\tau)}\Big[H(\tau-1) - H(\tau-\tau_\ell)\Big] + C_f\frac{\sqrt{\tau^2-\tau_\ell^2}\sqrt{1-\tau^2}}{(\tau_{bge}+\tau)(\tau_{bge}-\tau)}\Big[H(\tau-1)-H(\tau-\tau_\ell)\Big]\right\}$$
$$+ \frac{\pi}{2(1-k_e^4)}\left\{(1-C_f)\frac{\sqrt{\tau_{bge}^2-1}\Big(\sqrt{\tau_{bge}^2-1}+k_e^2\sqrt{\tau_{bge}^2-\tau_\ell^2}\Big)}{\tau_{bge}} + C_f\frac{\sqrt{\tau_{bge}^2-\tau_\ell^2}\Big(\sqrt{\tau_{bge}^2-1}+k_e^2\sqrt{\tau_{bge}^2-\tau_\ell^2}\Big)}{\tau_{bge}}\right\}\delta(\tau-\tau_{bge}) \tag{3.44}$$

The second term in (3.44) represents a singular impulsive disturbance contributed by the simple pole at $\zeta = -s_{bge}$, which is nondecaying and does not change in shape. Figure (5) displays the profiles of the surface disturbance for various electro-mechanical coupling coefficients k_e (the optical effect is too small to be shown). In addition, one may notice that in Figure (5) the transient response of electric displacement vanishes after acoustic SH wave arrives.

4. Lamb's problem with an adjoining vacuum half space

(a) Equal-light-speed approximation

In reality, the piezoelectric space is usually in contact with other dielectric spaces. In this section, we consider the problem of the piezoelectric half space that is abutted with an adjacent vacuum half space (Figure(6)). Based on the formulations in section 2, the following wave propagation problem is considered,

$$\nabla^2 w - \frac{1}{c_s^2}\frac{\partial^2 w}{\partial t^2} = 0\ ,\ x_2 > 0 \tag{4.1}$$

$$\nabla^2 \psi - \frac{1}{c_\ell^2}\frac{\partial^2 \psi}{\partial t^2} = 0\ ,\ x_2 > 0 \tag{4.2}$$

$$\nabla^2 \tilde{\phi} - \frac{1}{c_0^2}\frac{\partial^2 \tilde{\phi}}{\partial t^2} = 0\ ,\ x_2 < 0 \tag{4.3}$$

where $\tilde{\phi}$ is the electrical potential in the free space, and $c_0 > c_\ell > c_s$ ($s_0 < s_\ell < s_s$). The following mixed boundary value problem describes the general mixed type of line sources that are placed between the piezoelectric half space and vacuum half space.

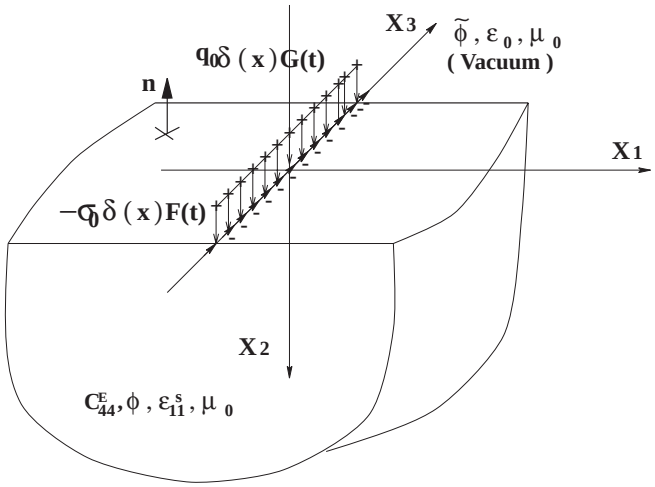

Figure 6.
Lamb's problem with an adjoining vacuum half space

$$\sigma_{23}(x_1, 0, t) = -\sigma_0 \delta(x_1) F(t) \tag{4.4}$$

$$E_1(x_1, 0, t) = \tilde{E}_1(x_1, 0, t) \tag{4.5}$$

$$D_2(x_1, 0, t) - \tilde{D}_2(x_1, 0, t) = -q_0 \delta(x_1) G(t) \tag{4.6}$$

Here, the anti-plane mechanical line load and the in-plane electrical line load are simultaneously applied onto the interface.

Applying the double Laplace transforms to the wave equations (4.1)–(4.3), one may find the following convergence solutions

$$\hat{w}^*(\zeta, x_2, p) = A(\zeta, p)\exp(-pa(\zeta)x_2)\ ,\ a(\zeta) := \sqrt{s_s^2 - \zeta^2}\ ; \tag{4.7}$$

$$\hat{\psi}^*(\zeta, x_2, p) = B(\zeta, p)\exp(-pe(\zeta)x_2)\ ,\ \beta(\zeta) := \sqrt{s_\ell^2 - \zeta^2}\ ; \tag{4.8}$$

$$\hat{\tilde{\phi}}^*(\zeta, x_2, p) = C(\zeta, p)\exp(pf(\zeta)x_2)\ ,\ f(\zeta) := \sqrt{s_0^2 - \zeta^2}\ . \tag{4.9}$$

The transformed boundary conditions at $x_2 = 0$,

$$\tilde{c}_{44}\frac{\partial \hat{w}^*}{\partial x_2} + e_{15}\frac{\partial \hat{\psi}^*}{\partial x_2} = -\sigma_0 F^*(p); \tag{4.10}$$

$$-\Big(\frac{e_{15}}{\epsilon_{11}^s}C_f\frac{\partial \hat{w}^*}{\partial x_1} + \frac{\partial \hat{\psi}^*}{\partial x_1}\Big) = -\frac{\partial \hat{\tilde{\phi}}^*}{\partial x_1}; \tag{4.11}$$

$$e_{15}(1 - C_f)\frac{\partial w^*}{\partial x_2} - \epsilon_{11}^s\frac{\partial \hat{\psi}^*}{\partial x_2} + \epsilon_0\frac{\partial \hat{\tilde{\phi}}^*}{\partial x_2} = -q_0 G^*(p), \tag{4.12}$$

yield the relationships among unknown image functions $A(\zeta, p)$, $B(\zeta, p)$, and $C(\zeta, p)$:

$$\begin{cases} \tilde{c}_{44}\alpha(\zeta)A(\zeta, p) + e_{15}e(\zeta)B(\zeta, p) = \sigma_0\dfrac{F^*(p)}{p} & (a) \\[2ex] \dfrac{e_{15}}{\epsilon_{11}^s}C_f A(\zeta, p) + B(\zeta, p) = C(\zeta, p) & (b) \\[2ex] e_{15}(1 - C_f)\alpha(\zeta)A(\zeta, p) - \epsilon_{11}^s e(\zeta)B(\zeta, p) - \epsilon_0\gamma(\zeta, p)C(\zeta) = q_0\dfrac{G^*(p)}{p} & (c) \end{cases} \tag{4.13}$$

Solving the above system of algebraic equations yields

$$A(\zeta, p) = \Big[\frac{\sigma_0 F^*(p)}{p} + \Big(\frac{e_{15}e(\zeta)}{\epsilon_{11}^s e(\zeta) + \epsilon_0 f(\zeta)}\Big)\frac{q_0 G^*(p)}{p}\Big]\Big[\frac{\epsilon_{11}^s e(\zeta) + \epsilon_0 f(\zeta)}{\bar{c}_{44}\epsilon_{11}^s e(\zeta) + \tilde{c}_{44}\epsilon_0 f(\zeta)}\Big] \cdot \Big[a(\zeta) - k_e^2\frac{\epsilon_0 f(\zeta)}{\bar{c}_{44}\epsilon_{11}^s e(\zeta) + \tilde{c}_{44}\epsilon_0 f(\zeta)}e(\zeta)\Big]^{-1} \tag{4.14}$$

$$B(\zeta, p) = \frac{e_{15}(1 - C_f)a(\zeta) - (e_{15}C_f/\epsilon_{11}^s)\epsilon_0 f(\zeta)}{\epsilon_{11}^s e(\zeta) + \epsilon_0 f(\zeta)}A(\zeta, p) - \frac{q_0 G^*(p)/p}{(\epsilon_{11}^s\beta(\zeta) + \epsilon_0 f(\zeta))} \tag{4.15}$$

$$C(\zeta, p) = \frac{e_{15}(1 - C_f)a(\zeta) + e_{15}C_f e(\zeta)}{\epsilon_0 e(\zeta) + \epsilon_{11}^s f(\zeta)}A(\zeta, p) - \frac{q_0 G^*(p)/p}{(\epsilon_{11}^s e(\zeta) + \epsilon_0 f(\zeta))} \tag{4.16}$$

By examining the expressions (4.14)–(4.16) closely, one may find that the algebraic structures of these image kernel functions are somewhat complicated, and the physical meaning of the expressions is not all clear.

Since the image function $A(\zeta, p)$ is the transformed displacement $\hat{w}^*(x_1, 0, p)$, it is then an "acoustic image". One may note that both mechanical line source as well as electrical line source attribute their influences on the image function $A(\zeta, p)$, which is the piezoelectric coupling effect that we expect. Shown by (4.15) and (4.16), the image kernel functions $B(\zeta, p), C(\zeta, p)$ have two parts: (a) acoustics part, which is associated with the kernel function $A(\zeta, p)$; and (b) electric part, which is solely credited to electrical line sources, and the electro-mechanical coupling is broken here.

To make the ensuing inversion process manageable, the following approximation is adopted:

Assumption 4.1. (Equal-light-speed approximation). *Based on above observations and the fact that $c_\ell, c_0 >> c_s$, the optical effect on acoustic wave is always negligible; thus, in "acoustic image" function $A(\zeta, p)$ and in the acoustic parts of image functions $B(\zeta, p)$ and $C(\zeta, p)$, we take*

$$\frac{e(\zeta)}{f(\zeta)} = \frac{\sqrt{s_\ell^2 - \zeta^2}}{\sqrt{s_0^2 - \zeta^2}} \approx 1 \ . \tag{4.17}$$

This implies that at acoustic end, one cannot distinguish the difference between the different light speeds in different dielectric media. □

It should be noted that this approximation is not applied to the electric part of the image functions $B(\zeta, p), C(\zeta, p)$.

Let $c_{44}^\epsilon := (\bar{c}_{44}\epsilon_{11}^s + \tilde{c}_{44}\epsilon_0)/(\epsilon_{11}^s + \epsilon_0)$. After simplification, the expressions (4.14)–(4.16) take a succinct form

$$A(\zeta, p) = \Big[\frac{\sigma_0 F^*(p)}{c_{44}^\epsilon p} + \frac{e_{15}}{\epsilon_0 + \epsilon_{11}^s}\frac{q_0 G^*(p)}{c_{44}^\epsilon p}\Big]\frac{a(\zeta) + k_v^2 e(\zeta)}{(1 - k_v^4)(s_{bgv}^2 - \zeta^2)} \tag{4.18}$$

$$\begin{aligned} B(\zeta, p) = &\Big[e_{15}(1 - C_f)a(\zeta) - \Big(\frac{e_{15}}{\epsilon_{11}^s} f\Big)\epsilon_0 f(\zeta)\Big]\frac{A(\zeta, p)}{\epsilon_{11}^s e(\zeta) + \epsilon_0 f(\zeta)} \\ &- \frac{q_0(G^*(p)/p)}{(\epsilon_{11}^s e(\zeta) + \epsilon_0 f(\zeta))} \end{aligned} \tag{4.19}$$

$$\begin{aligned} C(\zeta, p) = &\Big[e_{15}(1 - C_f)a(\zeta) + e_{15} C_f e(\zeta)\Big]\frac{A(\zeta, p)}{\epsilon_{11}^s e(\zeta) + \epsilon_0 f(\zeta)} \\ &- \frac{q_0(G^*(p)/p)}{(\epsilon_{11}^s e(\zeta) + \epsilon_0 f(\zeta))} \end{aligned} \tag{4.20}$$

where $k_v := k_e\sqrt{\dfrac{\tilde{c}_{44}\epsilon_0}{\bar{c}_{44}\epsilon_0+\tilde{c}_{44}\epsilon_{11}^s}}$, $s_{bgv} := \sqrt{\dfrac{s_s^2-k_v^4 s_\ell^2}{1-k_v^4}}$, and $c_{bgv}=1/s_{bgv}$.

Again, as $c_\ell \to \infty$, $(s_\ell \to 0)$,

$$k_v^2 \to \frac{{e_{15}}^2}{\bar{c}_{44}\epsilon_{11}^s}\frac{\epsilon_0}{\epsilon_0+\epsilon_{11}^s}$$
$$c_{bgv} \to c_s\sqrt{1-k_v^4}$$

which recovers the classical expression of Bleustein-Gulyaev wave speed, that is travelling through the interface between piezoelectric medium and vacuum space (Bleustein [1968], Gulyaev [1969], and Maugin [1983]).

Transient wave solutions

To this end, we are in a position to discuss the transient waves that are excited by mixed type (mechanical/electrical) line sources. Choose the following Cagniard-de Hoop inversion paths as shown in Figure (7):

$$\Gamma_a:\ \zeta_{\alpha\pm}=\frac{1}{r}\Big[-t\cos\theta\pm i\sin\theta\sqrt{t^2-s_s^2r^2}\Big];\ s_s r\le t<\infty \tag{4.21}$$

$$\Gamma_{ae}:\ \zeta_{ae\pm}=\frac{1}{r}\Big[-t\cos\theta\pm \sin\theta\sqrt{s_s^2r^2-t^2}\Big]\pm i\epsilon_{ae};\ t_{ae}\le t<s_s r \tag{4.22}$$

$$\Gamma_e:\ \zeta_{e\pm}=\frac{1}{r}\Big[-t\cos\theta\pm i\sin\theta\sqrt{t^2-s_\ell^2r^2}\Big];\ s_\ell r\le t<\infty \tag{4.23}$$

$$\Gamma_{ef}:\ \zeta_{\beta\gamma\pm}=\frac{1}{r}\Big[-t\cos\theta\pm \sin\theta\sqrt{s_\ell^2r^2-t^2}\Big]\pm i\epsilon_{ef};\ t_{ef}\le t<s_\ell r \tag{4.24}$$

$$\Gamma_f:\ \zeta_{f\pm}=\frac{1}{r}\Big[-t\cos\theta\pm i\sin\theta\sqrt{t^2-s_0^2r^2}\Big];\ s_0 r\le t<\infty \tag{4.25}$$

where $t_{ae}=\sqrt{s_s^2-s_\ell^2}x_2+s_\ell x_1$, $t_{ef}=\sqrt{s_\ell^2-s_0^2}x_2+s_0x_1$, and $\epsilon_{ab},\epsilon_{ef}$ are the radius of small circles at the tip of inversion paths $\Gamma_{\alpha\beta}$ and $\Gamma_{\beta\gamma}$ respectively.

It can be further derived that

$$\frac{\partial\zeta_{a\pm}}{\partial t}=\pm i\frac{a(\zeta_{a\pm})}{\sqrt{t^2-s_s^2r^2}}\ ;\ \alpha(\zeta_{\alpha\pm})=\frac{\sin\theta}{r}t\pm i\frac{\cos\theta}{r}\sqrt{t^2-s_s^2r^2} \tag{4.26}$$

$$\frac{\partial\zeta_{ae\pm}}{\partial t}=\mp\frac{a(\zeta_{ae\pm})}{\sqrt{s_s^2r^2-t^2}}\ ;\ a(\zeta_{ae\pm})=\frac{\sin\theta}{r}t\pm\frac{\cos\theta}{r}\sqrt{s_s^2r^2-t^2} \tag{4.27}$$

$$\frac{\partial\zeta_{e\pm}}{\partial t}=\pm i\frac{a(\zeta_{e\pm})}{\sqrt{t^2-s_\ell^2r^2}}\ ;\ a(\zeta_{\beta\pm})=\frac{\sin\theta}{r}t\pm i\frac{\cos\theta}{r}\sqrt{t^2-s_\ell^2r^2} \tag{4.28}$$

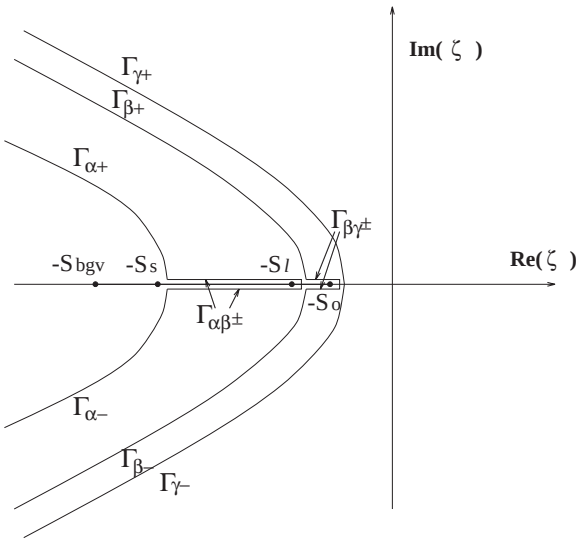

Figure 7.
Cagniard-de Hoop inversion paths for the Lamb's problem within vacuum environment

$$\frac{\partial \zeta_{ef\pm}}{\partial t} = \mp \frac{a(\zeta_{ef\pm})}{\sqrt{s_\ell^2 r^2 - t^2}} \; ; \; a(\zeta_{ef\pm}) = \frac{\sin\theta}{r} t \pm \frac{\cos\theta}{r}\sqrt{s_\ell^2 r^2 - t^2} \tag{4.29}$$

$$\frac{\partial \zeta_{f\pm}}{\partial t} = \pm i \frac{a(\zeta_{f\pm})}{\sqrt{t^2 - s_0^2 r^2}} \; ; \; a(\zeta_{f\pm}) = \frac{\sin\theta}{r} t \pm i \frac{\cos\theta}{r}\sqrt{t^2 - s_0^2 r^2} \tag{4.30}$$

Remark 4.1. At above, there are two supplement inversion paths: $\Gamma_{ae\pm}$ and $\Gamma_{ef\pm}$, in order to circumvent branch cuts caused by $e(\zeta)$ and $f(\zeta)$. The physical interpretations of the supplement paths are: the integral along $\Gamma_{ae\pm}$ represents an electroacoustic head wave, which is similar to the one discussed in section 3, and the integral along $\Gamma_{ef\pm}$ represents a purely electric head wave. These head waves only occur in specific regions, because they are generated by incident electric waves grazing through the surface, and then propagate to the interior at certain angles. The electroacoustic head wave occurs in the region

$$0 \le \theta \le \theta_{cr}^{ae} \text{ and } \pi \le \theta \le \pi - \theta_{cr}^{ae} \tag{4.31}$$

where $\theta_{cr}^{ae} = \cos^{-1}\Big(\frac{s_\ell}{s_s}\Big)$. The purely electric head wave occurs in the region that

$$0 \le \theta \le \theta_{cr}^{ef} \text{ and } \pi \le \theta \le \pi - \theta_{cr}^{ef} \tag{4.32}$$

where $\theta_{cr}^{ef} := \cos^{-1}\Big(\frac{s_0}{s_\ell}\Big) = \cos^{-1}\Big(\frac{\epsilon_0}{\epsilon_{11}^s}\Big)$. The specific regions for both head waves are schematically illustrated in Figure (8). In Figure (8), the region marked as

H_{ea} is the region affected by electroacoustic head wave, and region marked as H_e is the region disturbed by the purely electric head wave. □

Consider the impulsive line sources, i.e. $F(t) = \delta(t)$. Let $\bar{\sigma_0} = \sigma_0 + q_0 e_{15}/(\epsilon_{11}^s + \epsilon_0)$. The analytical solutions can then be expressed in closed form:

$$\begin{aligned} w^\delta(x_1,x_2,t) = \frac{1}{\pi}\Big(\frac{\bar{\sigma_0}}{c_{44}^\epsilon(1-k_v^4)}\Big)\Bigg\{ & Re\Big[\frac{a(\zeta)+k_v^2 e(\zeta)}{(s_{bgv}-\zeta)(s_{bgv}+\zeta)}\frac{a(\zeta)}{\sqrt{t^2-s_s^2r^2}}\Big]\Big|_{\zeta\in\Gamma_{a+}} \\ & \cdot H(t-s_s r) - Im\Big[\frac{a(\zeta)+k_v^2 e(\zeta)}{(s_{bgv}-\zeta)(s_{bgv}+\zeta)}\frac{a(\zeta)}{\sqrt{s_s^2r^2-t^2}}\Big]\Big|_{\zeta\in\Gamma_{ae+}} \\ & \cdot \Big(H(t-t_{ae}) - H(t-s_s r)\Big)\Bigg\} \end{aligned} \tag{4.33}$$

$$\begin{aligned} \psi^\delta(x_1,x_2,t) = \frac{1}{\pi}\frac{\bar{\sigma_0}}{c_{44}^\epsilon(1-k_v^4)}\Bigg\{ & Re\Big[\Big(e_{15}(1-C_f)a(\zeta) - \Big(\frac{e_{15}}{\epsilon_{11}^s}C_f\Big)\epsilon_0 f(\zeta)\Big) \\ & \cdot \Big(\frac{a(\zeta)+k_v^2\beta(\zeta)}{(s_{bge}^2-\zeta^2)}\frac{e(\zeta)}{\epsilon_{11}^s e(\zeta)+\epsilon_0 f(\zeta)}\Big)\Big]\Big|_{\zeta\in\Gamma_{e+}}\frac{H(t-s_\ell r)}{\sqrt{t^2-s_\ell^2r^2}} \\ & - Im\Big[\Big(e_{15}(1-C_f)a(\zeta) - \Big(\frac{e_{15}}{\epsilon_{11}^s}C_f\Big)\epsilon_0 f(\zeta)\Big) \\ & \Big(\frac{a(\zeta)+k_v^2 e(\zeta)}{(s_{bgv}^2-\zeta^2)}\Big)\Big(\frac{e(\zeta)}{\epsilon_{11}^s e(\zeta)+\epsilon_0 f(\zeta)}\Big)\Big]\Big|_{\zeta\in\Gamma_{ef+}}\Big(\frac{H(t-t_{ae})-H(t-s_s r)}{\sqrt{s_\ell^2r^2-t^2}}\Big)\Bigg\} \\ & - \frac{q_0}{\pi}\Bigg\{ Re\Big[\frac{e(\zeta)}{\epsilon_{11}^s e(\zeta)+\epsilon_0 f(\zeta)}\Big]\Big|_{\zeta\in\Gamma_{e+}}\frac{H(t-s_\ell r)}{\sqrt{t^2-s_\ell^2r^2}} \\ & - Im\Big[\frac{e(\zeta)}{\epsilon_{11}^s e(\zeta)+\epsilon_0 f(\zeta)}\Big]\Big|_{\zeta\in\Gamma_{ef+}}\frac{H(t-t_{ef})-H(t-s_\ell r)}{\sqrt{s_\ell^2r^2-t^2}}\Bigg\} \end{aligned} \tag{4.34}$$

and

$$\begin{aligned} \tilde{\phi}(x_1,x_2,t) = \frac{1}{\pi}\frac{\bar{\sigma_0}}{c_{44}^\epsilon(1-k_v^4)}\Bigg\{ & Re\Big[\Big(e_{15}(1-C_f)a(\zeta) + \Big(\frac{e_{15}}{\epsilon_{11}^s}C_f\Big)\epsilon_{11}^s e(\zeta)\Big) \\ & \cdot \Big(\frac{a(\zeta)+k_v^2 e(\zeta)}{s_{bgv}^2-\zeta^2}\Big)\Big(\frac{f(\zeta)}{\epsilon_{11}^s e(\zeta)+\epsilon_0 f(\zeta)}\Big)\Big]\Big|_{\zeta\in\Gamma_{f+}}\frac{H(t-s_0 r)}{\sqrt{t^2-s_0^2r^2}}\Bigg\} \\ & - \frac{q_0}{\pi}\Bigg\{ Re\Big[\frac{f(\zeta)}{\epsilon_{11}^s e(\zeta)+\epsilon_0 f(\zeta)}\Big]\Big|_{\zeta\in\Gamma_{f+}}\frac{H(t-s_0 r)}{\sqrt{t^2-s_0^2r^2}}\Bigg\} \end{aligned} \tag{4.35}$$

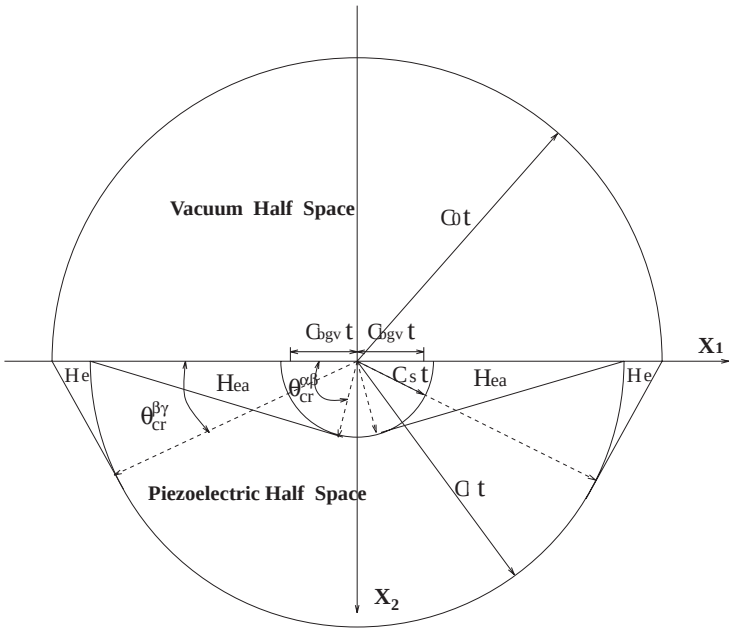

Figure 8.
Transient waves propagate on the piezoelectric half space

It would be interesting to examine the transient responses on the interface due to the mixed, impulsive line sources. Let

$$\tau_0 := \frac{s_0}{s_\ell} \ , \tag{4.36}$$

$$\tau_{bgv} := \frac{s_{bgv}}{s_s} \ , \tag{4.37}$$

The displacement response on the surface, $(x_2 = 0)$, takes the following dimensionless form

$$\frac{c_{44}^{\epsilon}\pi|x_1|}{\bar{\sigma_0}c_s} w^{\delta}(x_1, 0, t) = \frac{-1}{1-k_v^4} \left\{ \frac{\sqrt{\tau^2-1}H(\tau-1)}{(\tau_{bgv}-\tau)(\tau_{bgv}+\tau)} + \frac{k_v^2\sqrt{\tau^2-\tau_\ell^2}H(\tau-\tau_\ell)}{(\tau_{bgv}-\tau)(\tau_{bgv}+\tau)} \right\} \tag{4.38}$$

which is very similar to the displacement solution obtained in section 3. As a matter of fact, in Eq. (3.42), let $k_e \to k_v$, $\sigma_0 \to \bar{\sigma}_0$ and $\tau_{bge} \to \tau_{bgv}$; one recovers (4.38), which is another reason why Lamb's problem with shielded surface is a good bench mark problem, because it represents an intrinsic characteristic of Lamb's problem for piezoelectric materials.

Nevertheless, unlike the Lamb's problem with shielded surface, one may notice that here both mechanical and electrical loads are responsible for surface displacement disturbance, and the parameter $\bar{\sigma_0}$ reveals how the electro-mechanical coupling interplays. In practice, one can certainly adjust the ratio between mechanical

load and electrical load to either enhance or suppress the surface displacement disturbance.

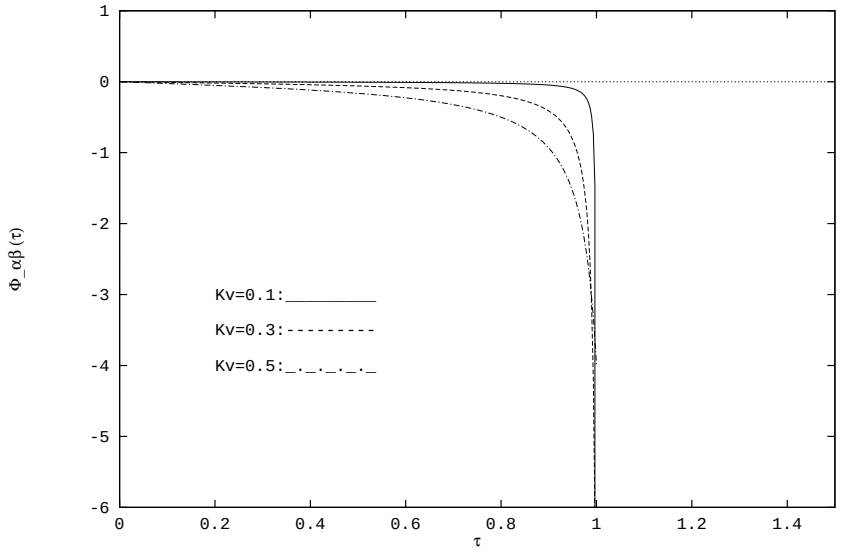

Figure 9.
Transient response of electroacoustic head wave on the free surface:
$\left(\Phi_{\alpha\beta}(\tau) := \frac{\epsilon_{11}^s c_{44}^e \pi |x_1|}{e_{15}\bar{\sigma}_0 c_s}\phi_{eah}^{\delta}(x_1,0,t)\right)$;

The solution of electrical potential, on the other hand, is quite different from the solution of the Lamb's problem with shielded surface. Unlike the electrical potential solution obtained in section 3, in which the electrical potential on the surface is always zero as prescribed by the boundary condition, there is a rich complexity of electrical potential disturbance on the interface; it consists of several parts in general:

$$\phi^{\delta}(x_1,0,t) = \phi_a^{\delta}(x_1,0,t) + \phi_{eah}^{\delta}(x_1,0,t) + \phi_e^{\delta}(x_1,0,t) + \phi_{eh}^{\delta}(x_1,0,t) \tag{4.39}$$

where the subscript "eh" is referred to as the contribution by a purely electric head wave.

Let

$$\epsilon_p := \frac{{\epsilon_{11}^s}^2 + \epsilon_{11}^s\epsilon_0 + {\epsilon_0}^2}{\epsilon_{11}^s + \epsilon_0} \tag{4.40}$$

$$s_p := \sqrt{\mu_0\epsilon_p}\ ,\ \left(c_p = \frac{1}{s_p}\right) \tag{4.41}$$

$$\tau_p := \frac{s_p}{s_s} \tag{4.42}$$

$$\varepsilon := \frac{\epsilon_{11}^s}{\epsilon_0} \tag{4.43}$$

The different electrical potential responses on the surface are given as follows:

$$\begin{aligned}\phi_a^\delta(x_1,0,t) = &-\Big(\frac{e_{15}}{\epsilon_{11}^s}C_f\Big)\frac{\bar{\sigma_0}}{c_{44}^\epsilon(1-k_v^4)}\Big(\frac{c_s}{\pi|x_1|}\Big)\\ &\cdot\left(\frac{\sqrt{\tau^2-1}+k_v^2\sqrt{\tau^2-\tau_\ell^2}}{(\tau_{bgv}+\tau)(\tau_{bgv}-\tau)}H(\tau-1)\right)-\Big(\frac{\bar{\sigma_0}}{c_{44}^\epsilon(1-k_v^4)}\Big)\\ &\cdot\Big(\frac{c_s}{\pi|x_1|}\Big)\Big(\frac{e_{15}}{\epsilon_0}\Big)\left[\frac{k_v^2(1-C_f)\sqrt{\tau^2\tau_\ell^2}-(C_f/\varepsilon)\sqrt{\tau^2-\tau_0^2}}{(\tau_{bgv}+\tau)(\tau_{bgv}-\tau)}\right]\\ &\cdot\frac{\sqrt{\tau^2-1}H(\tau-1)}{\epsilon_{11}^s\sqrt{\tau^2-\tau_\ell^2}+\epsilon_0\sqrt{\tau^2-\tau_0^2}}\end{aligned} \tag{4.44}$$

$$\begin{aligned}\phi_{eah}^\delta(x_1,0,t) = &-\Big(\frac{e_{15}}{\epsilon_{11}^s}C_f\Big)\frac{k_v^2\bar{\sigma}_0}{c_{44}^\epsilon(1-k_v^4)}\Big(\frac{c_s}{\pi|x_1|}\Big)\\ &\cdot\frac{\sqrt{\tau^2-\tau_\ell^2}\Big(H(\tau-\tau_\ell)-H(\tau-1)\Big)}{\tau_{bgv}^2-\tau^2}\end{aligned} \tag{4.45}$$

$$\phi_{e1}^\delta(x_1,0,t) = -\frac{q_0c_s}{\pi|x_1|}\cdot\frac{H(\tau-\tau_\ell)}{\epsilon_{11}^s\sqrt{\tau^2-\tau_\ell^2}+\epsilon_0\sqrt{\tau^2-\tau_0^2}} \tag{4.46}$$

$$\begin{aligned}\phi_{e2}^\delta(x_1,0,t) = &-\frac{e_{15}\bar{\sigma}_0}{c_{44}^\epsilon(1-k_v^4)}\Big(\frac{c_s}{\pi|x_1|}\Big)\\ &\cdot\left\{\Big(\frac{(1-C_f)(\tau^2-1)-(k_v^2C_f/\varepsilon)\sqrt{\tau^2-\tau_0^2}\sqrt{\tau^2-\tau_\ell^2}}{(\tau_{bgv}+\tau)(\tau_{bgv}-\tau)}\Big)\right.\\ &\left.\cdot\Big(\frac{H(\tau-\tau_\ell)}{\epsilon_{11}^s\sqrt{\tau^2-\tau_\ell^2}+\epsilon_0\sqrt{\tau^2-\tau_0^2}}\Big)\right\}\end{aligned} \tag{4.47}$$

$$\begin{aligned}\phi_{eh}^\delta(x_1,0,t) = &\Big(\frac{c_s}{\pi|x_1|}\Big)\Big(\frac{\epsilon_0}{{\epsilon_{11}^s}^2-{\epsilon_0}^2}\Big)\\ &\cdot\left\{\Big(\frac{e_{15}\bar{\sigma}_0}{c_{44}^\epsilon(1-k_v^4)}\Big)\Big((1-C_f)\sqrt{1-\tau^2}+C_f\sqrt{\tau_\ell^2-\tau^2}\Big)\right.\\ &\left.\cdot\left(\frac{\sqrt{1-\tau^2}+k_v^2\sqrt{\tau_\ell^2-\tau^2}}{\tau_{bgv}^2-\tau^2}\right)-q_0\right\}\frac{\sqrt{\tau^2-\tau_0^2}}{\tau_p^2-\tau^2}\\ &\cdot(H(\tau-\tau_0)-H(\tau-\tau_\ell))\end{aligned} \tag{4.48}$$

It is interesting to note that on the surface the electric waves at optical speed, $\phi_e^\delta(x_1,0,t)$ and ϕ_{eh}^δ, are solely dependent on electrical line source q_0, whereas electroacoustic waves, $\phi_a^\delta(x_1,0,t)$ and $\phi_{eah}^\delta(x_1,0,t)$, can be excited by both line sources.

In Figure (9) and (10), the transient responses of electroacoustic head wave ϕ_{eah}^δ, transverse electric wave $\phi_{e1}^\delta(x_1,0,t)$ and $\phi_{e2}^\delta(x_1,0,t)$ on the surface are plotted for comparison. Figure (9) shows that the surface disturbance of electroacoustic head wave reaches to an abyss around $\tau = 1$, because τ_{bgv} is very close to 1, whereas the surface disturbance of the electric wave $\phi_{e1}^\delta(x_1,0,t)$ reaches another abyss around $\tau = 0$, since τ_ℓ is very small.

5. Conclusions

In this paper, a notion of quasi-hyperbolic approximation is introduced for a class of transversely isotropic piezoelectric materials to restore hyperbolicity in the simplified Maxwell-Christoffel equations. The newly derived governing equations then furnish a more accurate formulation than classical formulation based on the quasi-static approximation, and it enables us to study the transient problem of piezoelectric media by using established mathematical methods.

Two types of Lamb's problem under mixed line sources are solved. The analytical results obtained here provide useful information to explain how transient waves propagating on the surface of a piezoelectric medium, such as the structures of electroacoustic head wave and purely electric head wave, and the disturbance effect of electroacoustic surface wave, etc.

The wave solutions obtained have a quantitative accuracy at acoustic range, whereas the wave solutions at optical range are only qualitative in nature, because of the overall "quasi-hyperbolic" approximation as well as the "equal-light-speed" approximation at the acoustic end. Nevertheless, it has become apparent that the "quasi-static" approximation does discard some crucial information for both electric wave as well as acoustic wave ! It is then suggested that discretion should be taken when using "quasi-static" approximation in transient problems of piezoelectric media.

The significance of this approach is multitude, because a large class of wave propagation problems in piezoelectric materials can be solved by following virtually the same procedure proposed here, such as the scattering and diffraction problems, inverse problems, as well as dynamic crack propagation problems in piezoelectric media.

References

[1] Achenbach, J.D., *Wave Propagation in Elastic Solids*, North-Holland Pub., Amsterdam/ London 1973.

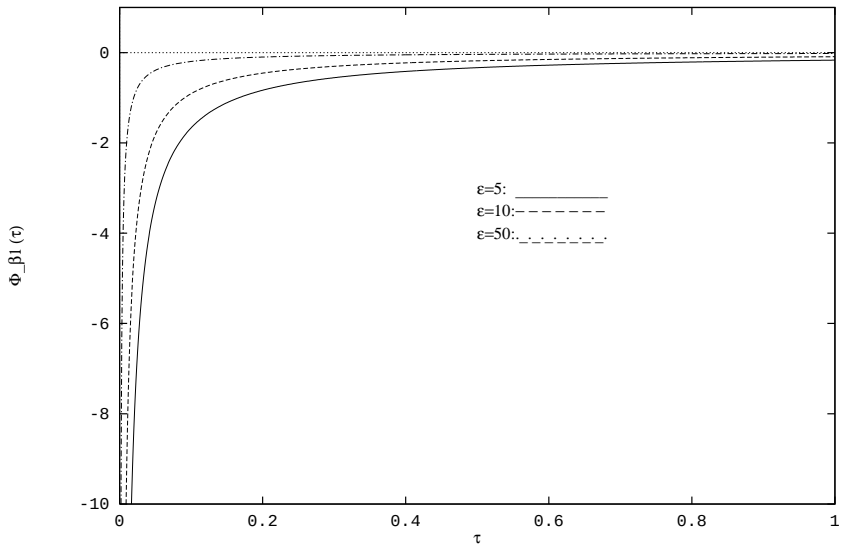

(a)

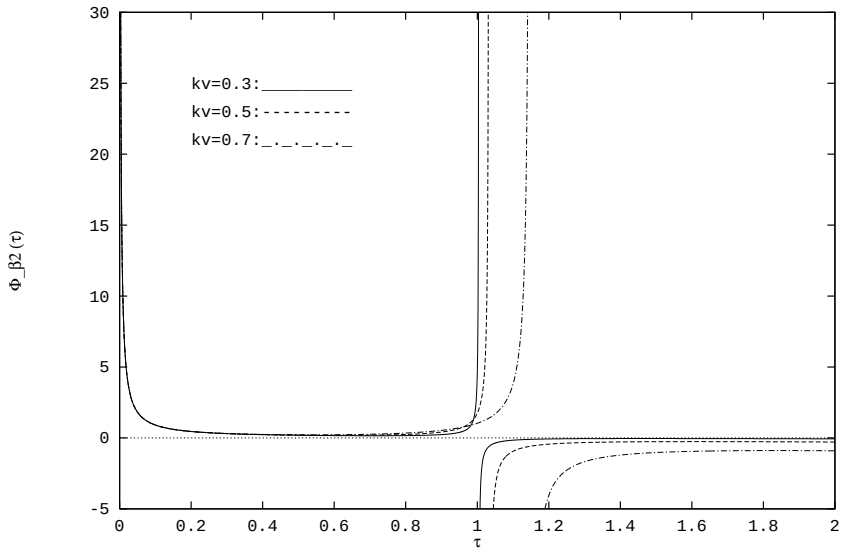

(b)

Figure 10.
Transient response of electrical potentials on the free surface: (a) Electric wave : $(\Phi_{e1}(\tau) := \frac{\pi|x_1|\epsilon_0}{q_0 c_s}\phi^{\delta}_{e1}(x_1,0,t)$ and $\varepsilon := \frac{\epsilon^s_{11}}{\epsilon_0}$. (a) Electric wave : $(\Phi_{e2}(\tau) := \frac{\pi|x_1|\epsilon_0 c^{\epsilon}_{44}}{\bar{\sigma_0} e_{15} c_s}\phi^{\delta}_{e2}(x_1,0,t)$ and $\varepsilon = 10$.

[2] Brock, L. M. and Achenboch, J. D., Extension of an interface under influence of transient waves. *Int. J. Solids and Structures* **9** (1973), 53–67.
[3] Auld, B. A., *Acoustic Fields and Waves in Solids*, Vol. 1 & Vol. 2nd Ed. Robert E Krieger Pub., Malabar, Florida 1990ab; 1st Ed. John & Wiley & Sons, New York 1973ab.
[4] Bleustein, J. L., A new surface wave in piezoelectric materials. *Appl. Phys. Lett.* **13** (1968), 412–413.
[5] Cady, W. G., *Piezoelectricity*, McGraw-Hill, New York 1946.
[6] Cagniard, L., *Reflection and Refraction of Progressive Seismic Waves*, Gauthier-Villars, Paris 1939.
[7] Currie, J. and Currie, P., *Compte Rendus* 1881 p. 1137.
[8] Felsen, L. B. and Marcuvitz, N., *Radiation and Scattering of Waves*, IEEE Press, Piscataway, NJ 08855 1994
[9] Fredericks, R. W., Diffraction of an elastic pulse in a loaded half-space, *J. Acoust. Soc. Am.* **33** (1961), 17–22.
[10] Gulyaev, Y. V., Electroacoustic surface waves in solids. *Soviet Physics JETP* **9** (1969), 37-38.
[11] de Hoop, A. T., A modification of Cagniard's method for solving seismic pulse problems. *Appl. Sci. Res.* **B8** (1960), 349-360.
[12] Jackson, J. D., *Classical Electrodynamics*, John Wiley & Sons, New York 1974.
[13] Lamb, H., On the propagation of tremors over the surface of an elastic solid. *Phil. Trans. Roy. Soc. (London)* **A203** (1903), 1-42.
[14] Li, S. and Mataga, P. A., Dynamic crack propagation in piezoelectric materials. Part I: electrode solution. *J. Mech. Phys. Solids* **44** (1996), 1799-1830.
[15] Li, S. and Mataga, P. A. Dynamic crack propagation in piezoelectric materials. Part II: vacuum solution. *J. Mech. Phys. Solids* **44** (1996), 1831-1866.
[16] Li, S., The electromagneto-acoustic surface wave in a piezoelectric medium: the Bleustein-Gulyaev mode. *J. Appl. Phys.* **80** (1996), 5264-5269.
[17] Lin, Y. and Wang, C. and Ying, C. F., Electromagnetic acoustic head waves in piezoelectric media. *Appl. Physs Lett.* **55** (1989), 434-436.
[18] Maugin, G. A., Elastic surface waves with transverse horizontal polarization. In: *Advances in Applied Mechanics*, Vol. **23** Ed. by Yih, C. S., pp. 373–434, Academic Press, New York 1983.
[19] Miklowitz, J., *The Theory of Elastic Waves and Waveguides*, North-Holland Pub. Amsterdam 1978.
[20] Parton, V. Z. and Kudryatvsev, B. A., *Electromagnetoelasticity*, Gordon & Beach, New York 1988.
[21] Rao, S. S. and Sunar, M., Piezoelectricity and its use in disturbance sensing and control of flexible structures: a survey. *Appl. Mech. Rev.* **47** (1994), 113-123.
[22] Tiersten, H. F., *Linear Piezoelectric Plate Vibrations*, Plenum Press, New York 1969.
[23] Toupin, R. A., The elastic dielectric. *J. Rat. Mech. Anal.* **5** (1956), 849-915.
[24] Toupin, R. A., A dynamical theory of elastic dielectric. *Int. J. Eng. Sci.* **1** (1963), 101-126.
[25] Voigt, W., *Annalen der Physik* **67** (1899), 345-365.

Shaofan Li, Department of Mechanical Engineering
McCormick School of Engineering and Applied Science
Northwestern University, Evanston, Illinois, IL60208, U.S.A.

(Received: December 18, 1998)

Appendix A: Product Decomposition of $BG(\zeta)$

This appendix outlines the derivation of the product decomposition of the Bleustein-Gulyaev function $BG(\zeta) := a(\zeta) - k_e^2 e(\zeta)$. This factorization provides the essential ingredient in solving the related Wiener-Hopf equations .

The expression of interest is

$$BG(\zeta) := a(\zeta) - k_e^2 e(\zeta) = (1 - k_e^4)\frac{(s_{bge} - \zeta)(s_{bge} + \zeta)}{a(\zeta) + k_e^2 e(\zeta)} \tag{1}$$

Factorize

$$a(\zeta) + k_e^2 e(\zeta) = (1 + k_e^2)\sqrt{s_{bge}^2 - \zeta^2}K(\zeta) \tag{2}$$

where

$$K(\zeta) := \frac{a(\zeta) + k_e^2 e(\zeta)}{(1 + k_e^2)\sqrt{s_{bge}^2 - \zeta^2}} \ . \tag{3}$$

where $K(\zeta) \to 1$ as $|\zeta| \to \infty$.

We then seek the product decomposition $K(\zeta) = K_+(\zeta)K_-(\zeta)$. It is usually convenient to express the product decomposition in an additive form, namely,

$$\log K(\zeta) = \log K_+(\zeta) + \log K_-(\zeta) = \frac{1}{2\pi i}\oint_C \frac{\log K(z)}{z - \zeta}dz \tag{4}$$

where C is the integration contour shown in Figure (11) and both $\log K_+(\zeta)$ and $\log K_-(\zeta)$ are sectionally analytic functions.

Define

$$\Theta(\zeta) := \arg\Big[K(\zeta)\Big]$$

By using the Cauchy principal value, it can be readily shown that along the contour $\mathbf{C}_+$ in Figure (11)

$$\Theta(\zeta) = \begin{cases} \pm\dfrac{\pi}{2}\ ; & -s_{bge} < Re(\zeta) < -s_s\ , \quad Im(\zeta) = \pm 0 \ \ (a) \\ \pm\arctan\{\Xi(\zeta)\}\ . & -s_s < Re(\zeta) < -s_\ell\ , \quad Im(\zeta) = \pm 0 \quad (b) \end{cases} \tag{5}$$

where

$$\Xi(\zeta) := \left\{\frac{k_e^2\sqrt{(\zeta - s_\ell)(\zeta + s_\ell)}}{\sqrt{(s_s - \zeta)(s_s + \zeta)}}\right\} \tag{6}$$

By Cauchy's integral theorem, it is not difficult to find that

$$K_+(\zeta) = \sqrt{\frac{s_s + \zeta}{s_{bge} + \zeta}}\exp\left\{-\frac{1}{\pi}\int_{s_\ell}^{s_s}\arctan\Big[\Xi(\eta)\Big]\frac{d\eta}{\eta + \zeta}\right\} \tag{7}$$

$$K_-(\zeta) = \sqrt{\frac{s_s - \zeta}{s_{bge} - \zeta}}\exp\left\{-\frac{1}{\pi}\int_{s_\ell}^{s_s}\arctan\Big[\Xi(\eta)\Big]\frac{d\eta}{\eta - \zeta}\right\} \tag{8}$$

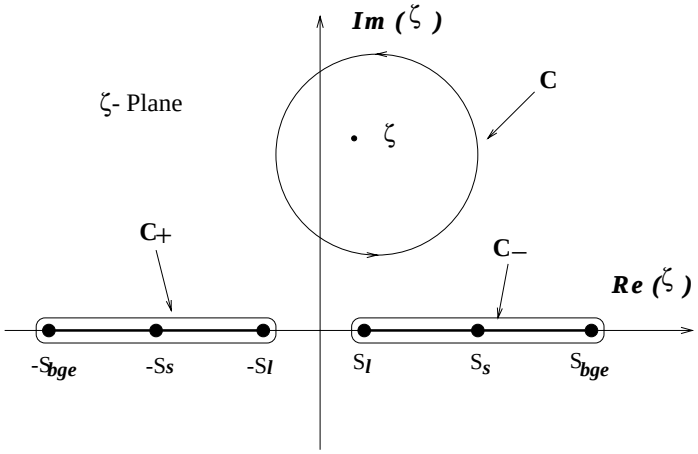

Figure 11.
Integration contours used for product decomposition of function $K(\zeta)$.

In accordance,

$$a(\zeta) + k_e^2 e(\zeta) = (1 + k_e^2)\sqrt{s_s^2 - \zeta^2}\,\mathcal{D}_+(\zeta)\mathcal{D}_-(\zeta) \tag{9}$$

where

$$\mathcal{D}_\pm(\zeta) := \exp\left\{-\frac{1}{\pi}\int_{s_\ell}^{s_s} \arctan\Big[\frac{k_e^2\sqrt{(\eta - s_\ell)(\eta + s_\ell)}}{\sqrt{(s_s - \eta)(s_s + \eta)}}\Big]\frac{d\eta}{\eta \pm \zeta}\right\} \tag{10}$$

Then the product decomposition for Bleustein-Gulyaev function $BG(\zeta)$ is obtained as

$$BG(\zeta) = (1 - k_e^2)\frac{(s_{bge} - \zeta)(s_{bge} + \zeta)}{\sqrt{(s_s - \zeta)(s_s + \zeta)}}\mathcal{S}_+(\zeta)\mathcal{S}_-(\zeta) \tag{11}$$

where $\mathcal{S}_\pm := 1/\mathcal{D}_\pm(\zeta)$.

Remark A.1. 1. From Figure 11, one can see that there are three branch points along each integration contour; this differs from the decomposition of the Rayleigh wave function used in the in-plane mode diffraction problem in an elastic medium (Fredricks [1961]) for which there are only two branch points along each integration contour.

2. The type of decomposition (9) is traditionally accomplished in a direct fashion (e.g. Brock & Achenbach [1973])

$$a(\zeta) + k_e^2 e(\zeta) = (1 + k_e^2)a(\zeta)\frac{a(\zeta) + k_e^2 e(\zeta)}{(1 + k_e^2)a(\zeta)} = (1 + k_e^2)a(\zeta)\mathcal{D}_+(\zeta)\mathcal{D}_-(\zeta) \tag{12}$$

Nonetheless, the elaboration here offers a detailed technical account.

3. There is a sign error in Li & Mataga [1996ab], in which

$$\mathcal{S}_\pm(\zeta) := \exp\left\{-\frac{1}{\pi}\int_{s_\ell}^{s_s} \arctan\Big[\frac{k_e^2\sqrt{(\eta - s_\ell)(\eta + s_\ell)}}{\sqrt{(s_s - \eta)(s_s + \eta)}}\Big]\frac{d\eta}{\eta \pm \zeta}\right\}$$

□